frontiers | Frontiers in Microbiology

TYPE Original Research
PUBLISHED 07 January 2025
DOI 10.3389/fmicb.2024.1491488

OPEN ACCESS

EDITED BY
Richard Allen White III,
University of North Carolina at Charlotte, United States

REVIEWED BY
Shingo Kato,
RIKEN BioResource Research Center (BRC), Japan
Yukari Maezato,
Solenis, United States
Timothy Rogers,
University of North Carolina at Charlotte, United States

*CORRESPONDENCE
Andreas Teske
✉ teske@email.unc.edu

RECEIVED 04 September 2024
ACCEPTED 18 December 2024
PUBLISHED 07 January 2025

CITATION
Hinkle JE, Chanton JP, Moynihan MA, Ruff SE and Teske A (2025) Complex bacterial diversity of Guaymas Basin hydrothermal sediments revealed by synthetic long-read sequencing (LoopSeq). *Front. Microbiol.* 15:1491488. doi: 10.3389/fmicb.2024.1491488

Complex bacterial diversity of Guaymas Basin hydrothermal sediments revealed by synthetic long-read sequencing (LoopSeq)

John E. Hinkle[1,2], Jeffrey P. Chanton[3], Molly A. Moynihan[4,5], S. Emil Ruff[4,5] and Andreas Teske[1]*

[1]Department of Earth, Marine and Environmental Sciences, University of North Carolina, Chapel Hill, NC, United States, [2]Department of Marine Science, University of Texas at Austin, Marine Science Institute, Port Aransas, TX, United States, [3]Department of Earth, Ocean and Atmospheric Science, Florida State University, Tallahassee, FL, United States, [4]Marine Biological Laboratory, The Ecosystems Center, Woods Hole, MA, United States, [5]Marine Biological Laboratory, The Bay Paul Center for Comparative Molecular Biology and Evolution, Woods Hole, MA, United States

Hydrothermal sediments host phylogenetically diverse and physiologically complex microbial communities. Previous studies of microbial community structure in hydrothermal sediments have typically used short-read sequencing approaches. To improve on these approaches, we use LoopSeq, a high-throughput synthetic long-read sequencing method that has yielded promising results in analyses of microbial ecosystems, such as the human gut microbiome. In this study, LoopSeq is used to obtain near-full length (approximately 1,400–1,500 nucleotides) bacterial 16S rRNA gene sequences from hydrothermal sediments in Guaymas Basin. Based on these sequences, high-quality alignments and phylogenetic analyses provided new insights into previously unrecognized taxonomic diversity of sulfur-cycling microorganisms and their distribution along a lateral hydrothermal gradient. Detailed phylogenies for free-living and syntrophic sulfur-cycling bacterial lineages identified well-supported monophyletic clusters that have implications for the taxonomic classification of these groups. Particularly, we identify clusters within *Candidatus* Desulfofervidus that represent unexplored physiological and genomic diversity. In general, LoopSeq-derived 16S rRNA gene sequences aligned consistently with reference sequences in GenBank; however, chimeras were prevalent in sequences as affiliated with the thermophilic *Candidatus* Desulfofervidus and *Thermodesulfobacterium*, and in smaller numbers within the sulfur-oxidizing family *Beggiatoaceae*. Our analysis of sediments along a well-documented thermal and geochemical gradient show how lineages affiliated with different sulfur-cycling taxonomic groups persist throughout surficial hydrothermal sediments in the Guaymas Basin.

KEYWORDS

LoopSeq, 16S rRNA, sulfur-cycling bacteria, sulfur cycle, Guaymas Basin, hydrothermal sediments

Introduction

The Guaymas Basin is a marginal rift basin in the Gulf of California that is characterized by the coexistence of hydrothermal vents and cold seeps. Unlike many other regions with hydrothermal vents, Guaymas Basin is subject to relatively high sediment accumulation rates (Calvert, 1966). Basaltic sills, freshly emplaced into organic-rich sediments, drive the hydrothermal circulation of hydrocarbons, sulfide, and nutrient-rich fluids (Einsele et al.,

1980; Lizarralde et al., 2011). Abundant energy and organic carbon sources (De la Lanza-Espino and Soto, 1999) sustain highly active and very diverse microbial communities in Guaymas Basin sediments (Pérez Castro et al., 2021; Teske et al., 2021). Carbon sources are likely to shift throughout hydrothermal gradients in the sediments. Aromatic hydrocarbons serve as widely available carbon sources for aromatic-degrading bacteria throughout surficial Guaymas Basin sediments (Mara et al., 2022; Gutierrez et al., 2015; Goetz and Jannasch, 1993). In contrast, alkanes and methane occur more abundantly near hydrothermally active "hot spots" (Song et al., 2021; McKay et al., 2016). The availability of alkanes and methane in hot sediments contributes to the evolution of thermotolerance and thermophily in several groups of alkane- and methane- oxidizing bacteria and archaea (Zehnle et al., 2023; Benito Merino et al., 2022). The upper limit of microbial hydrocarbon degradation is approximately 80°C, based on preferential microbial utilization of ^{12}C-substrates and concomitant accumulation of ^{13}C-enriched substrates below this temperature (Song et al., 2021).

The complex microbial communities of Guaymas Basin sediments have been examined by numerous sequencing studies throughout the past two decades. Sequence-based surveys started with the use of near-full-length (~1,500 nucleotides) cloned PCR products (Teske et al., 2002), then progressed to high throughput pyrosequencing of very short (~80 nucleotides) 16S rRNA gene fragments (Ruff et al., 2015). More recent studies use high throughput sequencing methods that produce longer (~400–500 nucleotides) 16S rRNA gene fragments (Teske et al., 2019; Su et al., 2023). The abundance of sequence data obtained via different methods makes the Guaymas Basin an ideal model system to assess the performance of new next-generation sequencing technologies, such as LoopSeq.

LoopSeq is a high-throughput synthetic long-read sequencing method, which can generate near-full length gene sequences (Callahan et al., 2021). Studies using clone library construction and sequencing methods yield near full-length and high-quality sequences but are greatly limited by throughput and sequencing depth. Clone library-based methods are time consuming and only the most abundant microorganisms are usually detected. In turn, high throughput sequencing methods can yield tens of thousands of sequence reads, allowing to detect extremely rare organisms (Sogin et al., 2006). Yet, these reads are too short for high-resolution phylogenetic analyses and can only be used for relatively basic taxonomic identification. Short reads of 400–500 nucleotides can be used to construct phylogenies, but placement of unknown or poorly resolved lineages remains problematic, due to the limited information provided by short sequences and limited bootstrap support for phylogenetic branching patterns (Teske et al., 2019; Ramírez et al., 2021).

LoopSeq bridges this gap and allows investigators to obtain nearly full-length 16S rRNA gene sequences in high throughput, for costs comparable to short read amplicons. The combination of high throughput and nearly full-length sequences allows for thorough surveys of the diversity of known microbial lineages, as well as high-resolution phylogenetic placement of rare or poorly resolved microbial lineages even for highly diverse ecosystems, such deep-sea hydrothermal sediments. To date, marine hydrothermal sediments have not been targeted using LoopSeq. Previous environmental studies using LoopSeq have focused on environments of agricultural importance such as the soybean rhizosphere (Yu et al., 2022), sorghum rhizosphere (Chiniquy et al., 2021), and raw milk (Abellan-Schneyder et al., 2021). To test the capabilities and reliability of LoopSeq for complex and challenging marine sediment samples, Guaymas Basin is ideal because (i) the ecosystem is generally well understood, (ii) the microbial communities of its hydrothermal sediments are very diverse, (iii) the sediments are rich in organics that can be problematic for sequencing, e.g., hydrocarbons, and (iv) extensive 16S rRNA gene sequence databases are available to verify LoopSeq sequences against publicly available short read and full-length sequences.

Our analyses focus on sequences from well-established and phylogenetically well-documented sulfur-cycling bacterial groups as robust reference sequences that are available in public sequencing databases (i.e., NCBI GenBank), to validate the accuracy of LoopSeq as a foundation for future exploratory surveys, and to explore the diversity and spatial distribution of these sulfur-cycling bacteria. Archaeal lineages are less suitable for initial validation; apart from the well-described and locally dominant *Candidatus* Methanophagales (ANME-1) lineage, the extremely diverse and phylogenetically scattered archaeal lineages in Guaymas Basin (Teske et al., 2002) would complicate the authentication of LoopSeq-generated sequences.

Methods

Sampling

Guaymas Basin sites were visited and sampled with R/V *Atlantis*, human-occupied vehicle (HOV) *Alvin*, and autonomous underwater vehicle (AUV) *Sentry* during cruise AT37-06 (December 6–29, 2016). *Alvin* dives targeted previously explored sampling areas in the southern axial valley of Guaymas Basin (Teske et al., 2016), or newly identified sites found by AUV *Sentry*. Hydrothermal sediment samples (*Alvin* push cores) used in this study were obtained during *Alvin* Dive 4872 (Dec. 24, 2016) in the Cathedral Hill area (27°00.684 N/ 111°24.266 W) at 2014 m depth. The sample set covers a hydrothermal gradient from hot hydrothermally charged sediments covered with orange and white *Beggiatoaceae* mats to temperate bare sediment, within ~1 m distance (Figure 1). Core 4872–01 represents bare sediment that was not covered by a *Beggiatoaceae* mat, whereas Core 4872–06 was covered by a white *Beggiatoaceae* mat, and Core 4872–14 was covered by an orange *Beggiatoaceae* mat. Once the sediment cores

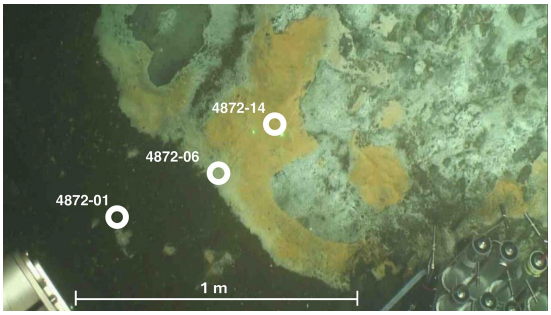

FIGURE 1
Seafloor image of sampling mat area at Dive 4872. Approximate location of push coring sites are labeled in white. Image courtesy of HOV *Alvin* Dive Team.

were returned to the surface, porewater profiles were collected using rhizons (Rhizosphere Research Products, Wageningen, The Netherlands). Then, these cores were divided into 3 cm sections and methane samples were collected by injecting 2 mL sediment plugs into 30 mL serum vials containing 2 mL of 1 M sodium hydroxide solution each. The serum vials were immediately sealed with thick rubber stoppers, crimped with aluminum seals, and stored at 4°C. The remaining sediment samples were frozen at −80°C by the shipboard science crew, and later used for DNA extraction shoreside.

Thermal profiles

Thermal profiles were measured in surficial sediments using *Alvin's* 50 cm heat flow probe.[1] The 50 cm probe contains thermal sensors every 10 cm, starting 5 cm below the attached plastic disk (the "puck") that limits probe penetration and rests on the seafloor once the probe was inserted. After 5 to 10 min of temperature reading stabilization, temperature readings were recorded.

Geochemical analyses

For sulfide analysis, 1 mL porewater subsamples were fixed with 0.1 mL of 0.1 M zinc acetate solution to preserve sulfide as zinc sulfide until analysis using the methylene blue method (Cline, 1969). For sulfate measurements, porewater samples were diluted in water (1:50) and analyzed using ion chromatography (Metrohm 930 Compact IC flex with Metrosep A PCC HC/4.0 preconcentration column, and Metrosep A Supp 5 Guard/4.0 chromatography column). Sulfate for the white and orange cores was measured by Wetland Biogeochemistry Analytical Services (WBAS) using ion chromatography on a Dionex ICS-1000 using a RFIC IonPac AS22 4 × 250 mm column and a RFIC IonPac AG22 Guard column 4 × 50 mm. The IC was calibrated using a 5-point standard curve and a minimum R^2 value of 0.999. The detection limit measured at 0.10 ppm sulfate. A check standard was made from a Dionex 7 anion standard (1,000 ppm) to a concentration of 15 ppm. An external Standard from HACH (100 ppm sulfate) was used to make a 20 ppm quality check standard. In general, quality checks were analyzed for 10% of the samples.

Porewaters from the Guaymas Basin were analyzed at WBAS for nitrate/nitrite (NO_x) and ammonium (NH_4^+) concentrations colorimetrically, using a Flow Solutions IV segmented flow Auto Analyzer from O.I Analytical, College Station, TX. The HCl-acidified samples were neutralized with sodium hydroxide (NaOH) before analysis. NO_x was determined using the cadmium reduction method and NH_4^+ was determined using the phenate method. Both nutrients were diluted to get their concentrations within the linear range of the auto analyzer. Quality control standards from certified stock standards (Environmental Research Associates), were analyzed every 15–20 samples.

For combined concentration and $\delta^{13}C$ analysis of methane, 2 mL sediment subsamples were added to 30 mL serum vials containing 2 mL of 1 M NaOH solution, sealed with thick butyl rubber stoppers, crimped with aluminum seals, and stored at 4°C. Since cores were retrieved unpressurized, outgassing may have particularly impacted the measurements of methane concentrations near and above saturation. After the cruise, the methane samples were analyzed by headspace gas chromatography-flame ionization detection (GC-FID) at Florida State University (Magen et al., 2014). Additionally, the gas samples were analyzed for $\delta^{13}CH_4$ by injecting 0.1 to 0.5 mL of sample into a gas chromatograph interfaced to a Finnigan MAT Delta S Isotope Ratio Mass Spectrometer inlet system as previously described (Chanton and Liptay 2000). Values are reported in the per mil (‰) notation relative to Vienna Pee Dee Belemnite (VPDB).

DNA extraction

DNA was extracted from Guaymas Basin sediment samples using a published protocol for soil DNA (Zhou et al., 1996). The extraction method was modified to optimize DNA recovery from deep-sea sediments. The detailed protocol can be found in the Supplementary Data Sheet 1.

LoopSeq sequencing

Sequencing libraries were prepared from extracted genomic DNA with the commercially available LoopSeq kits from Loop Genomics (Supplementary Data Sheet 2).[2] Synthetic long reads (SLRs) were constructed from the short-read sequencing reads using the standard Loop Genomics informatics pipeline and processed as previously described (Callahan et al., 2021). The method involves attaching two DNA tags: one Unique Molecular Identifier (UMI) to each unique "parent" DNA molecule and one sample-specific tag (i.e., a sample index) equally to all molecules in the same sample. Barcoded molecules are amplified, multiplexed, and each UMI is distributed intramolecularly to a random position within each parent molecule. Molecules are then fragmented into smaller units at the position of each UMI, creating a library of UMI-tagged fragments with an average length of 400 bp compatible with an Illumina sequencing platform run in PE150 mode (Callahan et al., 2021).

This protocol allows for the assembly of continuous 16S rRNA gene long reads from individual DNA molecules, providing sequencing data like classical long read sequencing methods but with much higher throughput. The terminal primers determine the extent of the 16S rRNA gene sequence yielded by this approach (27F, 5'-AGAGTTTGATCMTGGCTCAG-3′; 1492R, 5'-TACCTTG TTACGACTT-3′). LoopSeq can be performed on existing DNA sequencing instruments, and due to the chemistry and the tagging of individual molecules the method is semi-quantitative providing a major advantage toward other amplification-based methods.

We note that LoopSeq reconstructs a single long read from several short reads. Therefore, we define the resulting amplicon sequence variants (ASVs) as LoopSeq variants (L-ASVs) to

1 https://ndsf.whoi.edu/alvin/using-alvin/sampling-equipment/

2 https://go.elementbiosciences.com/16s-loopseq-user-guide

differentiate them from "traditional" ASVs that are essentially PCR amplicons.

Processing of 16S RNA gene amplicons

The statistical programming language R 4.2.1 (R Core Team, 2022) and the DADA2 (v. 1.20.0) bioinformatics package (Callahan et al., 2016), along with a LoopSeq suitable DADA2 workflow (Callahan et al., 2021) were used to analyze 16S rRNA gene sequences obtained by LoopSeq sequencing. This workflow is available at Github.[3] DADA2 creates ASVs (or LoopSeq variants (L-ASVs) in our case) by grouping together amplicon reads of the same sequence.

The function "removePrimers" was used to select for 16S rRNA amplicon sequences with both the forward and reverse primers and allowing a maximum mismatch of two base pairs, as reads lacking either primer do not represent the complete gene. The following parameters were used to filter the remaining sequences: a minimum length of 1,000 bp (minLen = 1,000), a maximum length of 2000 bp (maxLen = 2000), a minimum quality score of 3 (minQ = 3), a maximum expected error rate of 1 (maxEE = 1), and a maximum Ns of 0 (maxN = 0). These parameters may be used to filter reads without selecting for reads with a forward and reverse primer to capture long, but not complete genes. We found that 20.4% of reads that fulfilled the previously stated parameters lacked the forward/reverse primer. Only full-length gene sequences were kept in our analysis. The function "dereqFastq" was used to dereplicate reads. The function "learnErrors" was used with a band size of 32 (BAND_SIZE = 32) to learn error rates. The error estimate function was set to the PacBio Error Function. DADA2 was ran with a *p*-value cutoff of 1^{-10} (OMEGA_A = 1e-10), single detection (DETECT_SINGLETONS = TRUE), and a band size of 32 (BAND_SIZE = 32). The function "removeBimeraDenovo" (method = consensus) was used to remove chimeras. An overview of raw read processing is depicted in Supplementary Table 1.

The function "assignTaxonomy" was used to assign taxonomy using the Silva reference database (v138) (Quast et al., 2013). A total of 12,494 L-ASVs were identified. Figures depicting taxonomic distribution, alpha diversity, and beta diversity (Figure 2; Supplementary Figures 2, 3) were created using the R Phyloseq package (McMurdie and Holmes, 2013). All sequence reads were submitted to the NCBI Sequence Read Archive (BioProject: PRJNA1105367).

16S rRNA gene sequence phylogeny

We compared our L-ASV sequences against reference sequences obtained from the NCBI GenBank database. All sequences were aligned using Multiple Sequence Comparison by Log-Expectation (MUSCLE) in MEGA11 (Stecher et al., 2020). From these alignments, MEGA11 was used to construct minimum-evolution phylogenetic trees. MEGA11 provides the option to use the Kimura 2-parameter (K2P) model to calculate gene distances (Kimura, 1980). The K2P model is well-suited to clustering similar sequences, and stays close to empirically observed 16S rRNA gene distances (esp. for low sequence divergence <5%, common in our datasets) that form the basis for taxonomic recommendations (Stackebrandt and Goebel, 1994; Qin et al., 2014; Konstantinidis et al., 2017). The resulting phylogenies were checked by the aggregate of 1,000 bootstrap replicates (Rzhetsky and Nei, 1995; Felsenstein, 1985), in addition to cross-checking with published phylogenies for consistency. Bootstrap values greater than 70% are shown and NCBI GenBank accession numbers are provided on tip labels. Phylogenies were checked for consistency against independently derived phylogenies in relevant papers (Knittel et al., 2003; Salman et al., 2011; Schutte et al., 2018; Jochum et al., 2018; Krukenberg et al., 2016).

16S rRNA gene sequence distance matrices

Distance matrices corresponding to each phylogenetic tree are shown in Supplementary Data Sheet 3. The number of base substitutions between sequences are shown as a percentage (i.e., per 100 sites). Analyses were conducted using the Maximum Composite Likelihood model (Tamura et al., 2004). Each analysis involved all 16S rRNA gene sequences displayed in the corresponding phylogenetic tree. All ambiguous positions were removed for each sequence pair (pairwise deletion option). Evolutionary analyses were conducted in MEGA11 (Tamura et al., 2021; Stecher et al., 2020).

Results and discussion

Sediment characteristics

The color of Guaymas Basin *Beggiatoaceae* mats indicated the relative temperature of the underlying sediment as measured using the *Alvin* heat flow probe; orange mats covered hotter sediments and white mats covered comparatively cooler sediments (McKay et al., 2012). Temperature varied greatly with increasing sediment depth at the three sample sites (Figures 1, 3A). Temperatures at 40 centimeters below the seafloor (cmbsf) exceeded 100°C below the orange mat, reached 75°C below the white mat, and remained near 20°C in sediments without a *Beggiatoaceae* mat (Figure 3A).

Temperature considerably impacts microbial population density, and therefore the amount of DNA available for extraction. Measurable concentrations of DNA persisted the deepest (40 cmbsf) in Core 1, from bare sediment neighboring the warm mats. In contrast, DNA recovery is limited to surficial sediments (~ 20 cmbsf) in Core 14 from the hot center of the orange mat (Figure 3B.). Interestingly, the highest DNA yield (ca. 2.5 to 7 ug DNA/cm^3 sediment) are found within the upper ~6 cm of sediment in all three cores, indicating that the impact of hydrothermal activity extends beyond the *Beggiatoaceae* mats to the bare sediments of Core 1 (Figure 3B). Previous research in Guaymas Basin consistently reveals a very rapid decline in cell counts and 16S rRNA gene abundances with increasing depth and temperature in hot hydrothermal sediments (Meyer et al., 2013; Møller et al., 2018; Lagostina et al., 2021).

Micromolar concentrations of sulfide are observed throughout the bare sediment core, whereas the white and orange mat cores reach concentrations of sulfide up to 2 millimolar (Figure 3C). At the

3 https://github.com/moyn413/GuaymasLoopSeq/

10.3389/fmicb.2024.1491488

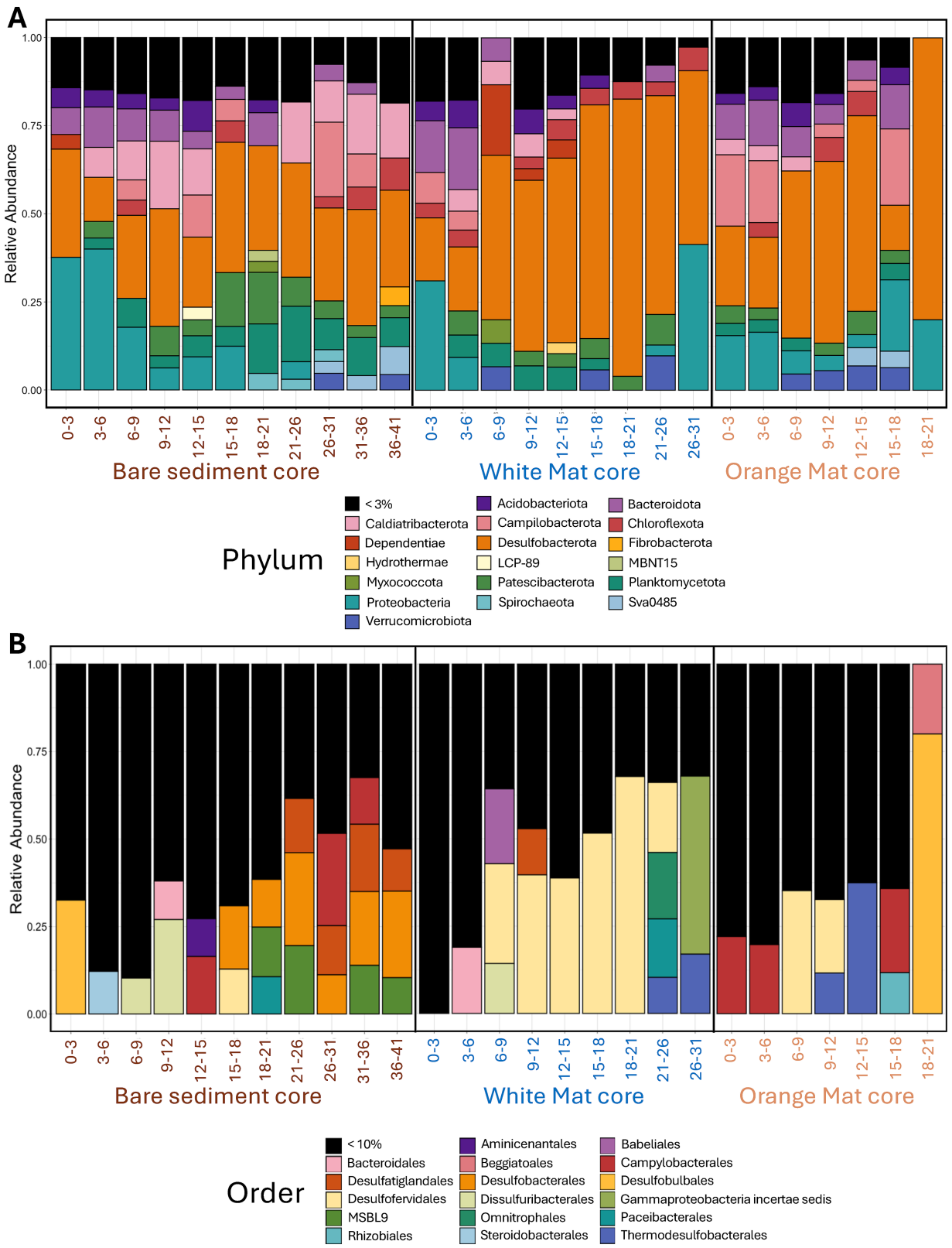

FIGURE 2
Stacked bar plots of **(A)** phylum-level and **(B)** order-level bacterial diversity. Phyla that comprise more than 3% of total sequence reads and Orders comprising more than 10% of total sequence reads are displayed. These percentage cutoffs were chosen to represent a balance between taxonomic resolution and figure legibility. The X-axis represents depth below seafloor (in centimeters) for the three sediments cores across the mat transect (bare sediment 4872–01, white mat 4872–06, orange mat 4872–14).

10.3389/fmicb.2024.1491488

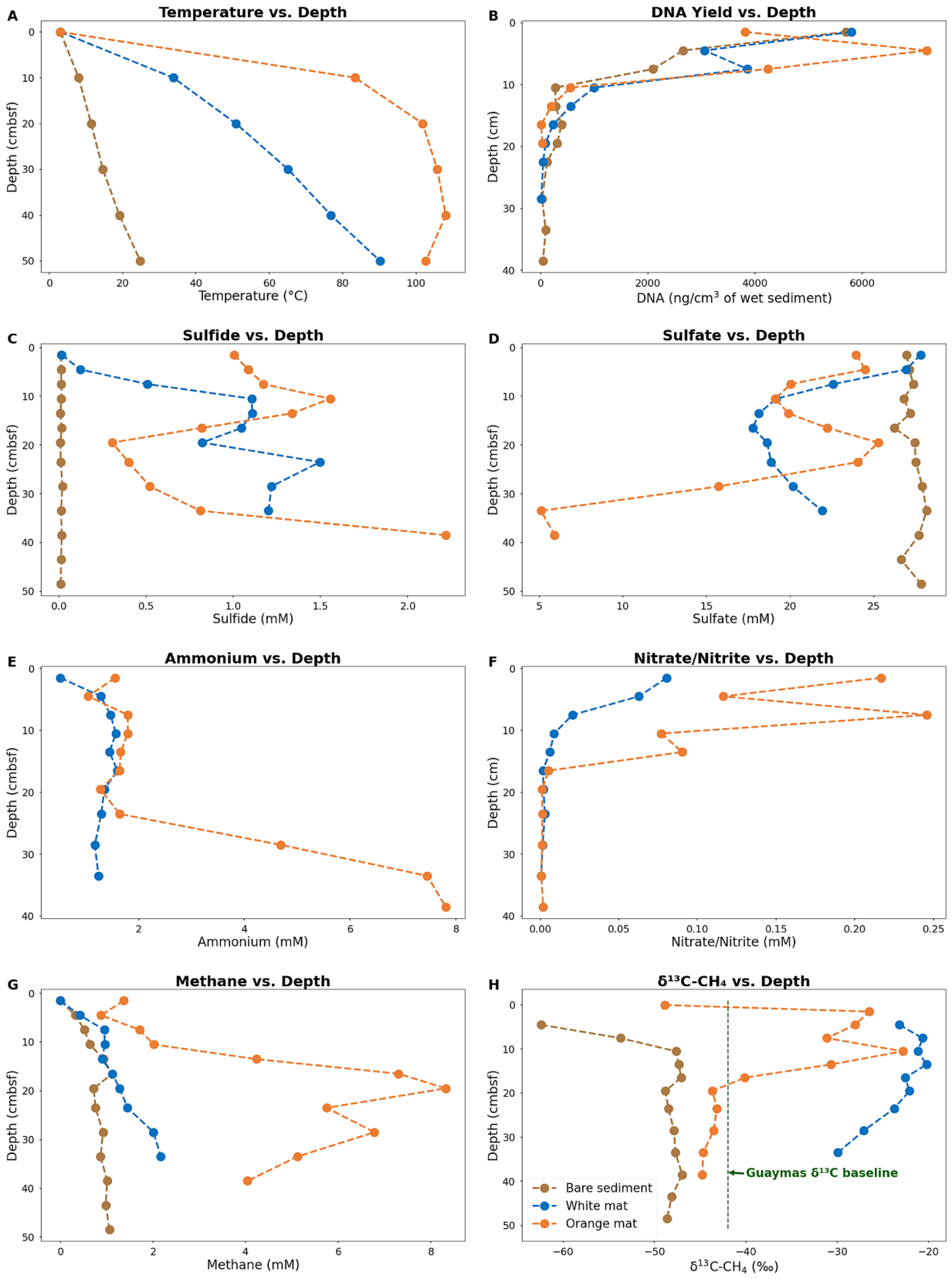

FIGURE 3
Plots of in-situ temperatures **(A)**, DNA concentrations **(B)** and geochemical parameters **(B–H)** for sediment cores. Sulfide **(C)** sulfate **(D)**, Ammonium **(E)**, and Nitrite/Nitrate **(F)** concentrations were obtained from porewater. Methane concentrations **(G)** and $\delta^{13}C$ values **(H)** were obtained from whole sediment. Ammonium and Nitrite/Nitrate concentrations are not available for the bare sediment site (Core 4872–01). Data for the bare sediment site (Core 4872–01) are plotted in brown. Data for the white mat site (Core 4872–06) are plotted in blue. Data for the orange mat site (Core 4872–14) are plotted in orange. Plotted data are available in Supplementary Table 2.

surface, sulfide concentrations are near zero for the bare sediment and white mat cores. In contrast, the orange mat core has elevated (~1 millimolar) sulfide levels at the surface, consistent with high hydrothermal flow in the mat center. Sulfate is abundant in all three cores, with depletion only occurring at ~32 cm and below in the orange mat core, indicating that hydrothermal circulation contributes to the replenishment of sulfate in surficial sediments (Figure 3D).

Ammonium is observed throughout our white and orange mat sediment cores (Figure 3E) Consistent with previous research, ammonium concentrations increase as temperature increases downcore (Ramírez et al., 2021). Ammonium in Guaymas Basin hydrothermal sediments is primarily derived from the thermal degradation of organic matter (Von Damm et al., 1985). Deep in the orange mat core, ammonium concentrations reach ~8 mM (Figure 3E), close to the ~10–15 mM concentrations observed in Guaymas Basin hydrothermal fluids (Von Damm et al., 1985).

Elevated nitrate/nitrite concentrations are observed in surficial mat covered sediments (Figure 3F). Bottom water concentrations of nitrate in Guaymas Basin are up to 50 μM (Winkel et al., 2014). Elevated nitrate levels (up to nearly 0.25 mM; Figure 3F) in mat-covered surficial sediments are at least in part due to damaged *Beggiatoaceae* mats leaking nitrate stored in their vacuoles into surficial sediments (Schutte et al., 2018).

High concentrations of methane are observed in all three cores (Figure 3G). A gradient of peak methane concentrations (~1 mM in the bare sediment core, ~2 mM in the white mat core, and ~ 8 mM in the orange mat core) illustrates the impact of hydrothermal fluids that are supersaturated in methane. High methane concentrations (multiple millimolar) are a characteristic feature of Guaymas Basin hydrothermal sediments, similar to those found at cold seep sites (Welhan, 1988; McKay et al., 2016; Song et al., 2021).

Hydrothermal methane in Guaymas Basin unmodified by microbial activity has a $\delta^{13}CH_4$ value of approximately −42 ‰ (McKay et al., 2016; Song et al., 2021). The preferential oxidation of $^{12}CH_4$ by methane-oxidizing archaea leads to the orange and white mat cores containing methane with a heavier carbon isotopic signature that is relatively enriched in ^{13}C, with values ranging from −30 to −20 ‰ (Figure 3H). The lighter carbon isotopic signature of methane throughout the bare sediment core and near the surface of the orange and white mat cores, indicates some contribution due to microbial methanogenesis (Figure 3H). The methanogens in these sediments include methylotrophs, which thrive in sulfate-replete sediments (Zhuang et al., 2018); numerous additional types of methanogens have been detected as well (Dhillon et al., 2005; Lever and Teske, 2015).

Sequencing profile

LoopSeq recovered nearly full-length sequences (Supplementary Figure 1, in Data Sheet 4) that affiliated with several phyla of heterotrophic bacteria, such as most *Proteobacteria*, *Desulfobacterota*, *Bacteroidota*, and *Chloroflexi* (Figure 2). These phyla have been detected by previous Guaymas Basin sequencing surveys using clone libraries of near full-length 16S rRNA genes (Teske et al., 2002; Dowell et al., 2016; McKay et al., 2016).

We analyzed the alpha diversity of each mat site using five measures (Observed, Chao1, Shannon, Simpson, and Inverse Simpson). We expected hydrothermal stress to influence alpha diversity based on previous research showing that alpha diversity decreases with increasing hydrothermal fluid temperature (Barosa et al., 2023) and with increasing sediment depth and temperature (Ramírez et al., 2021). However, we found no significant difference in alpha diversity between the three coring sites as indicated by the Kruskal-Wallis rank sum test (Supplementary Figure 2, Data Sheet 4). This unexpected result may reflect the previously observed high degree of habitat connectivity in Guaymas Basin sediments (Meyer et al., 2013), emerging from the coexistence of different electron acceptors and donors in non-consolidated sediments that undergo rapid hydrothermal pulses (McKay et al., 2016) and allow the coexistence of physiologically distinct microbial groups in surficial sediments (Engelen et al., 2021).

To explore potential differences in beta diversity, we created non-metric multi-dimensional scaling (NMDS) and dendrogram plots based on the Bray–Curtis dissimilarity method. Based on the dendrogram we highlighted a cluster of deeper samples (≥ 21 cmbsf) from the bare sediment site (Supplementary Figure 3, Data Sheet 4).

Sulfur-cycling lineages that frequently interface with hydrocarbon metabolism are present throughout surficial hydrothermal sediments in the Guaymas Basin (Figure 2). Numerous sulfate-reducing lineages (SEEP-SRB lineages, *Candidatus* Desulfofervidus) exist in syntrophic assemblages with methane- and alkane-oxidizing archaea (Knittel et al., 2003; Krukenberg et al., 2016), while other sulfate reducers (*Desulfatiglans*) perform terminal oxidation of hydrocarbons as free-living organisms (Teske et al., 2019). Sulfur-oxidizing *Beggiatoaceae* are known to assimilate methane-derived carbon (McKay et al., 2012). We performed phylogenetic analyses on these sulfur-cycling lineages to determine their intragroup diversity. Of 12,494 L-ASVs, 799 were identified as *Candidatus* Desulfofervidus, 585 as *Desulfatiglans*, 158 as SEEP-SRB2, 135 as SEEP-SRB4, and 29 as *Beggiatoaceae.*

Beggiatoaceae

The detection of *Beggiatoaceae* is an interesting test of LoopSeq capabilities. Previous efforts to generate full-length *Beggiatoaceae* sequences required collecting large amounts of individually prepared and cleaned filaments (McKay et al., 2012). Due to the size of individual *Beggiatoaceae* cells, they are outnumbered by other much smaller marine bacteria, complicating sequencing efforts and requiring high-throughput methods to overcome the ubiquitous presence of other marine bacterial groups. In our survey, all LoopSeq variants (L-ASV) identified as *Beggiatoaceae* matched reference sequences of the white or orange phylotype, with no additional phylotypes identified (Figure 4; Supplementary Figure 5, in Data Sheet 4). We note that light microscopy observations have revealed substantial diversity in the filament sizes of *Beggiatoaceae* (Nelson et al., 1989, Salman et al., 2013), indicative of further sequence diversity that remains to be detected. There is no evidence for introns within the 16S rRNA genes of Guaymas Basin *Beggiatoaceae,* although they have been observed in non-Guaymas Basin *Beggiatoaceae* (Salman et al., 2011; Salman et al., 2012). The LoopSeq primers coincide positionally with PCR primers previously used to amplify *Beggiatoaceae* sequences (Teske et al.,

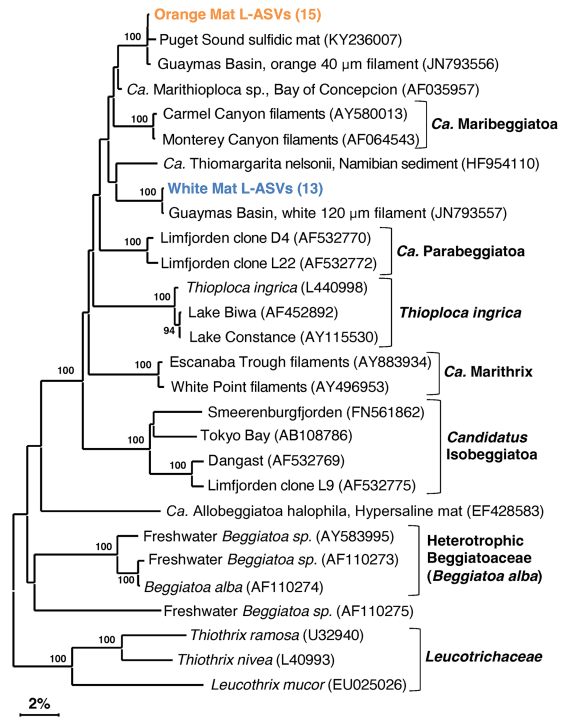

FIGURE 4
16S rRNA gene sequence based phylogenetic tree of *Beggiatoaceae* and related lineages. Bootstrap values greater than 70% are shown. Two distinct sequence types are highlighted in color, an orange filament cluster composed of L-ASVs from the orange mat site (4872–14) and a cluster composed of L-ASVs from the white mat site (4872–06), each with reference sequences obtained from GenBank. A version of this tree with expanded L-ASV clusters is available as Supplementary Figure 2.

2002; McKay et al., 2012), and in addition accommodate ambiguous nucleotide positions; therefore, primer mismatches can be ruled out. Recovered L-ASVs were generally found to be associated with surficial sediments underlying white and orange *Beggiatoaceae* mats. Some L-ASVs were found below the surface, resulting from the coring device pulling some of the long filaments down into the sediment column (Teske, 2009; Supplementary Figure 6 in Data Sheet 4).

Candidatus Desulfofervidus

In contrast to *Beggiatoaceae*, *Candidatus* Desulfofervidus sequences are often recovered in Guaymas Basin sequencing surveys (McKay et al., 2016; Dowell et al., 2016). *Ca.* Desulfofervidus is a sulfate-reducing syntrophic partner of methane- and alkane-oxidizing archaea (Laso-Pérez et al., 2016) with a thermal optimum of 50°C (Holler et al., 2011) to 60°C (Kniemeyer et al., 2007; Wegener et al., 2015). Although often observed as a syntroph, *Ca.* Desulfofervidus can also survive as a free-living hydrogenotroph without methane- or alkane-oxidizing partners (Krukenberg et al., 2016). *Ca.* Desulfofervidus is a phylogenetically narrow clade, as it is classified as its own family, order, and class-level lineage within the phylum Desulfobacterota (Waite et al., 2020). However, previous research has not examined the phylogenetic diversity within *Ca.* Desulfofervidus.

Our phylogeny identified several phylotypes of near-identical 16S rRNA gene sequences within *Candidatus* Desulfofervidus, each consisting of reference sequences from 50°C (Holler et al., 2011) or 60°C (Kniemeyer et al., 2007; Wegener et al., 2015) enrichments. All reference sequences were from Guaymas Basin, with no close matches from other sites. The close alignment of our sequences with established Guaymas Basin reference sequences attests to their quality. Our phylogeny supports the previous assertion of Krukenberg et al. (2016) that all *Ca.* Desulfofervidus lineages are closely related, since they form a well-defined 16S rRNA gene sequence cluster of approximately 98.5% sequence identity (Supplementary Data File 1, Sheet 2). The repeated detection of near-identical phylotypes within the *Ca.* Desulfofervidus cluster (Figure 5) implies the presence of unrecognized species diversity within *Ca.* Desulfofervidus.

We found sequences in GenBank that formed two deeply branching clusters with strong bootstrap support that are distinct from the major group of *Ca.* Desulfofervidus (Figure 5). These clusters were separated from the main group by sequence divergence up to 5.8% (Supplementary Data File 1, Sheet 2). The recovery of these sequences across independent studies at different vent sites suggests unrecognized microbial diversity related to *Ca.* Desulfofervidus. A previous metagenomic survey of Guaymas Basin hydrothermal sediments detected metagenome-assembles genomes (MAGs) branching between *Ca.* Desulfofervidus and *Thermodesulfobacteriaceae* (Dombrowski et al., 2018). Detailed analyses of these MAGs (labeled as B74_G16 and B4_G9) would reveal the genomic content and physiological potential of Desulfofervidus-affiliated lineages.

SEEP-SRB2

Like *Ca.* Desulfofervidus, SEEP-SRB2 sequences are often recovered in Guaymas Basin sequencing surveys (Dowell et al., 2016). Our survey recovered sequences from slightly below the surface to approximately 15 cmbsf. Unlike *Ca.* Desulfofervidus, SEEP-SRB2 sequences are recovered from diverse non-hydrothermal environments; cold seeps, salt lakes, coastal sediments, and estuaries (Kleindienst et al., 2014; Ruff et al., 2015). Despite its ecological importance as a syntrophic partner of methane and alkane oxidizers at cool and warm temperatures (enriched at 20°C and 37°C; Krukenberg et al., 2018), the internal phylogenetic structure of this group has not been examined in any detail.

Our SEEP-SRB2 phylogeny is largely comprised of a well-supported major cluster with ~97.5% sequence identity (Supplementary Data File 1, Sheet 3, equivalent to *Genus* level; Schloss and Handelsman, 2005). The closest cultured relatives of SEEP-SRB2, *Dissulfuribacter thermophilus* and *Dissulfurimicrobium hydrothermale*, are thermophilic sulfur disproportionators isolated from hydrothermal environments (Slobodkin et al., 2013; Slobodkin et al., 2016). These bacteria constitute separate lineages but share a deep branching point with SEEP-SRB2 (Figure 6). The distinctiveness of these lineages is further supported by sequence distances of up to 11% (Supplementary Data File 1, Sheet 3). Our 16S rRNA gene sequences indicate that SEEP-SRB2 would form a stand-alone group within

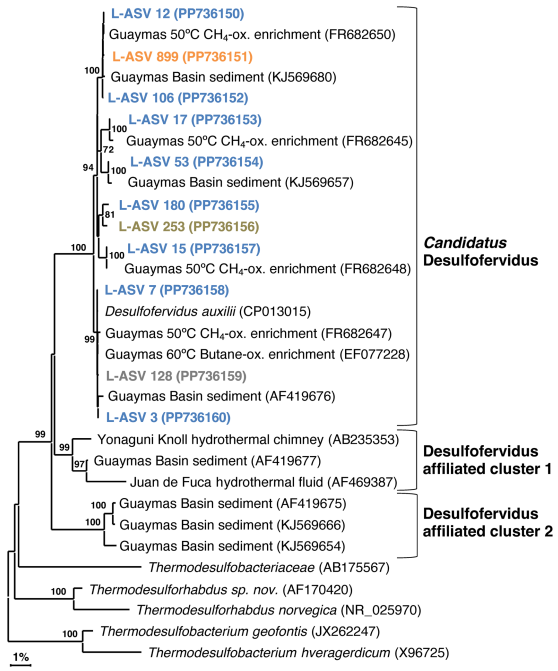

FIGURE 5
16S rRNA gene sequence based phylogenetic tree of *Candidatus* Desulfofervidus and related lineages. Bootstrap values greater than 70% are shown. NCBI GenBank accession numbers are provided in each tip label. L-ASV tip labels are color coded according to the site where the majority (2/3) of reads were recovered. This phylogenetic tree is based on shorter sequences where the first ~200 bp were discarded due to chimera issues. Brown = bare sediment, 4872–01; Blue = white mat site, 4872–06; Orange = orange mat, 4872–14; Gray = no site had a 2/3+ share of reads.

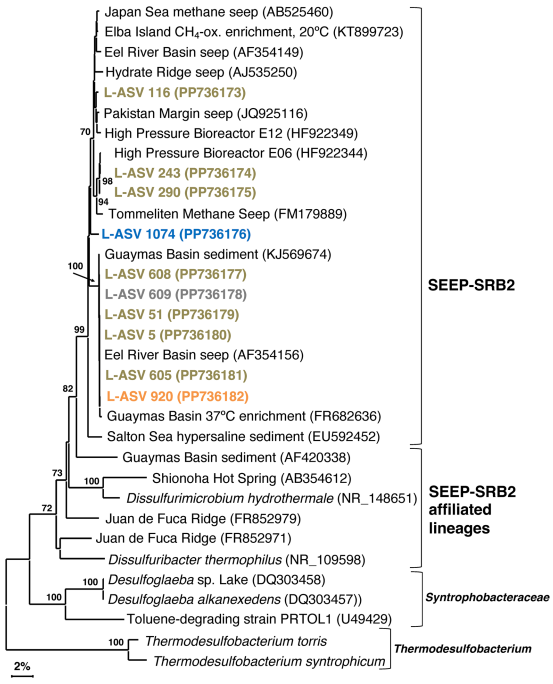

FIGURE 6
16S rRNA gene sequence based phylogenetic tree of SEEP-SRB2 and related lineages. Bootstrap values greater than 70% are shown. NCBI GenBank accession numbers are provided in each tip label. L-ASV tip labels are color coded according to the site where the majority (2/3) of reads were recovered. This phylogenetic tree is based on shorter sequences where the first ~200 bp were discarded due to chimera issues. Brown = bare sediment, 4872–01; Blue = white mat site, 4872–06; Orange = orange mat, 4872–14; Gray = no site had a 2/3+ share of reads. **Thermodesulfobacterium torris* 16S rRNA sequence was obtained from an annotated genome (BioSample ID: SAMN27514933). **Thermodesulfobacterium syntrophicum* 16S rRNA sequence was obtained from an annotated genome (BioSample ID: SAMN29995626).

Dissulfuribacteraceae (Waite et al., 2020). Further phylogenetic diversity that would fall between the pure culture examples (*Dissulfuribacter thermophilus* and *Dissulfurimicrobium hydrothermale*) and SEEP-SRB2 remains to be explored. Previously, the creation of a taxonomic family to comprise *Dissulfuribacter thermophilus* and *Dissulfurimicrobium hydrothermale* has been suggested (Slobodkin et al., 2013). Our phylogeny shows that such a group would also include SEEP-SRB2 (Figure 6).

SEEP-SRB4

In contrast to the syntrophic symbionts SEEP-SRB1 and SEEP-SRB2, SEEP-SRB4 has largely been overlooked since it was proposed 20 years ago (Knittel et al., 2003). FISH surveys indicate that SEEP-SRB4 is not a syntroph but occurs as individual free-living cells in cold seep sediments (Knittel et al., 2003). The closest cultured relatives of SEEP-SRB4 are non-thermophilic sulfur-disproportionating genera such as *Desulforhopalus* (Isaksen and Teske, 1996), *Desulfocapsa* (Finster et al., 1998), *Desulfofustis* (Friedrich et al., 1996), and the sulfate-reducing psychrophile *Desulfotalea* (Knoblauch et al., 1999). While SEEP-SRB2 has been enriched from Guaymas Basin sediments at 37°C (Krukenberg et al., 2018), there is currently no evidence that SEEP-SRB4 is moderately thermotolerant. We seek to test this assumption in our survey, checking the distribution of SEEP-SRB4 in surficial hydrothermal sediments. As with SEEP-SRB2, we seek to investigate the previously unrecognized phylogenetic diversity of SEEP-SRB4.

Our SEEP-SRB4 phylogeny depicts one major cluster with strong bootstrap support (100%) and > 98.9% sequence identity (Supplementary Data File 1, Sheet 4). This cluster contains several well-supported, phylogenetically narrow clusters (Figure 7). While the phylogeny shows a potential Guaymas Basin-specific subcluster of four sequences, the other subclusters contain globally distributed sequences from diverse cold seep sites and from Guaymas Basin.

The majority of L-ASVs for SEEP-SRB4 are retrieved from the top ~6 cm of the sediment across the entire lateral hydrothermal gradient (Supplementary Table 3). The preference for surficial sediments may be due to the abundance of elemental sulfur and polysulfides located there (Teske et al., 2016). A similar preference for surficial sediments with coexisting sulfate and sulfide was noted in the first study of SEEP-SRB4 (Knittel et al., 2003). SEEP-SRB4 bacteria seem to be able to colonize surficial hydrothermal sediments as long as in-situ temperatures remain relatively cool, similar to the strategy utilized by Guaymas Basin *Beggiatoaceae* (McKay et al., 2012).

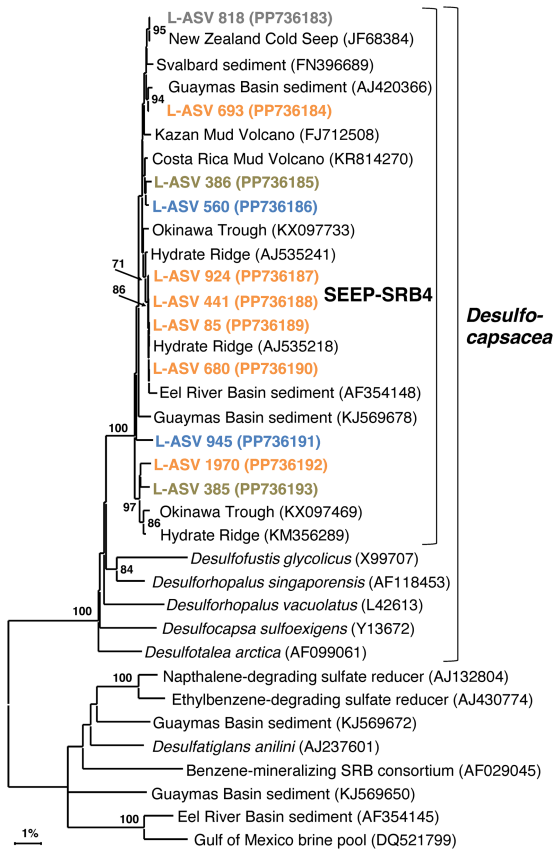

FIGURE 7
16S rRNA gene sequence based phylogenetic tree of SEEP-SRB4 and related lineages. Bootstrap values greater than 70% are shown. NCBI GenBank accession numbers are provided in each tip label. L-ASV tip labels are color coded according to the site where the majority (2/3) of reads were recovered. This phylogenetic tree is based on shorter sequences where the first ~200 bp were discarded due to chimera issues. Brown = bare sediment, 4872–01; Blue = white mat site, 4872–06; Orange = orange mat, 4872–14; Gray = no site had a 2/3+ share of reads.

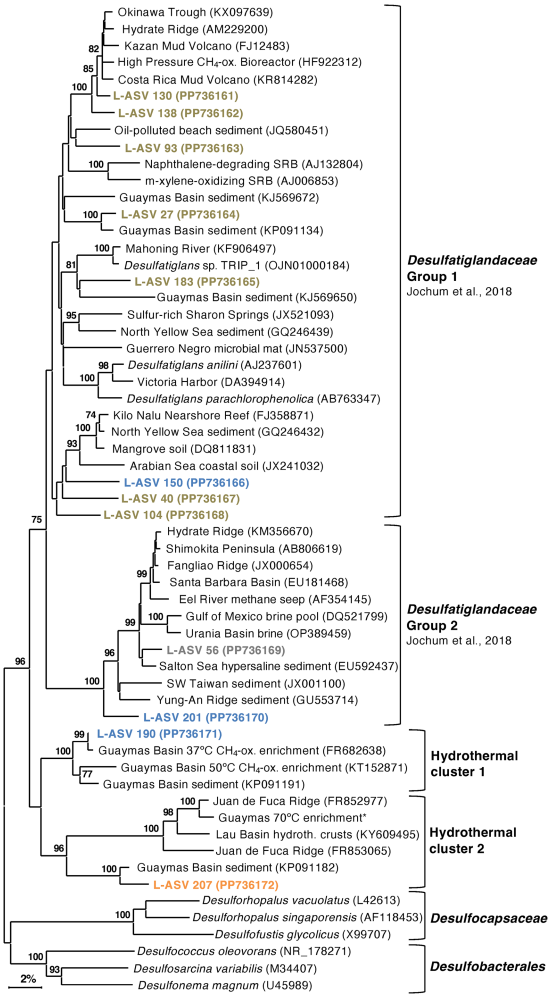

FIGURE 8
16S rRNA gene sequence based phylogenetic tree of *Desulfatiglans* and related lineages. Bootstrap values greater than 70% are shown. NCBI GenBank accession numbers are provided in each tip label. L-ASV tip labels are color-coded according to the site where the majority (2/3) of reads were recovered. This phylogenetic tree is based on shorter sequences where the first ~200 bp were discarded due to chimera issues. Brown = bare sediment, 4872–01; Blue = white mat site, 4872–06; Orange = orange mat, 4872–14; Gray = no site had a 2/3+ share of reads. The Guaymas 70°C enrichment sequence, marked with an asterisk (*), is from MAG 9 (B70, Benzene enrichment at 70°C) under BioProject PRJNA1013425.

Desulfatiglans

Desulfatiglandales is an order-level lineage within the phylum *Desulfobacterota* that contains polyaromatic degrading organisms, both isolated and uncultured species. The order and family level taxonomy are named after *Desulfatiglans annilini*, the first cultured representative (Suzuki et al., 2014). Sequences related to *Desulfatiglans* are often recovered in Guaymas Basin sequencing surveys (Ramírez et al., 2021; Dowell et al., 2016), including the shallow subsurface (Edgcomb et al., 2022). In contrast to the tightly clustered groups of SEEP-SRB2 and SEEP-SRB4, *Desulfatiglans* exhibits a greater degree of phylogenetic diversity.

Our Guaymas Basin sequences and almost all GenBank sequences were not closely related to cultured isolates that degrade polyaromatic and substituted-aromatic compounds (Figure 8). Even finding uncultured sequences that were closely related (>98% sequence identity) to some of our Guaymas Basin ASVs proved to be difficult. This could imply an undersampling of the natural diversity of *Desulfatiglans*, or their ongoing diversification and speciation. Previously, *Desulfatiglans* has been classified into two groups distinguished by genomic and physiological differences, Group 1 consisting of sulfate reducers and Group 2 consisting of dehalogenating subsurface bacteria (Jochum et al., 2018). Most of our L-ASVs belong to Group 1 and a few belong to Group 2.

Outside of these two groups, we found two well-supported hydrothermal clusters (Figure 8). The first cluster contained L-ASV 190 (predominately recovered from the white mat site), sequences from 37°C and 50°C enrichments of Guaymas Basin sediment (Kellermann et al., 2012; Wegener et al., 2015) and an environmental sequence from

Guaymas Basin hydrothermal sediment (McKay et al., 2016). The second cluster contained L-ASV 207 (predominately recovered from the orange mat site), a sequence from a *Desulfatiglans* MAG that was prevalent in a 70°C enrichment of Guaymas Basin sediment (Zehnle et al., 2023), and environmental sequences from diverse hydrothermal sediments (Li et al., 2014; Li et al., 2020). We examined these sequences via distance matrix analyses and find that these hydrothermal clusters are generally separated from other sequences by 11–12% sequence divergence (Supplementary Data File 1, Sheet 5).

In contrast to other sulfate reducers that occur in warm and hot Guaymas Basin sediments, we observed most of our *Desulfatiglans* L-ASVs in cool sediments, suggesting that they do not depend on methane and light hydrocarbons derived from hydrothermal fluids, and instead utilize polyaromatics (Schnell and Schink, 1991; Zehnle et al., 2023). Polyaromatics from hydrothermal oils are prevalent throughout Guaymas Basin sediments of diverse thermal regimes (Kawka and Simoneit, 1990), and *Desulfatiglans* appears to have evolved to utilize polyaromatics across the thermal spectrum, as suggested by its hydrothermal clusters.

Chimera issues

DADA2 detected chimeras in approximately 4% of our reads from a natural hydrothermal community. Previous research found structural errors (chimeras and introgressions) in approximately 2% of reads from a Zymo mock community (Callahan et al., 2021). Specifically, we found that LoopSeq produced chimeras in the majority of *Candidatus* Desulfofervidus sequences we examined. Segments of these sequences were entered into BLASTn, and we discovered that the chimeras consistently occurred in the first ~200 bp. BLASTn searches of the chimeric segments revealed their relation to other marine sediment bacteria such as *Chloroflexi*. The chimera breaks are located within the highly variable Helix 11 of the 16S rRNA gene (Van de Peer et al., 1996), and therefore appear to be secondary structure dependent. These issues with *Ca.* Desulfofervidus sequences were observed in samples across the DNA concentration range, from very high (4,240 ng/cm^3) to very low (0.5 ng/cm^3). Automated chimera identifying programs can have sensitivity issues when used with uncultured lineages that have poorly resolved phylogenies. We found that trimming off the first ~200 bp remedied the chimera issue, resulting in sequences with high alignment quality and > 97% identity to previously archived *Ca.* Desulfofervidus sequences available in GenBank.

LoopSeq recovered eight sequences identified by the DADA2 annotation pipeline as "*Thermodesulfobacterium*." Initial analysis of theses sequences showed that they were plagued with chimera and artifact issues, a potential consequence of low DNA yields from deep, hot samples. Two sequences were salvaged; one did not have chimera issues (L-ASV 12240), while the other was trimmed to only include the first ~340 bp (L-ASV 11484). These two sequences came from samples with low DNA concentrations (Sample 4872-06-08, 50 ng/cm^3 and Sample 4872-06-09, 12 ng/cm^3). These two sequences formed a Guaymas Basin specific cluster (Supplementary Figure 7) with the thermophilic ANME-1 syntroph *Thermodesulfobacterium torris* (Benito Merino et al., 2022) and a nearly identical hydrothermal sediment clone (McKay et al., 2016).

Conclusion

Our sequencing survey has shown that LoopSeq is a promising option for the high throughput long read sequencing of diverse microbial communities in hydrothermal sediments. The huge quantity of sequences yielded by LoopSeq allowed us to further resolve the fine scale phylogenetic structure of sulfur-cycling bacterial groups that are characteristic of Guaymas Basin hydrothermal sediments. The five well-supported clusters revealed in our *Ca.* Desulfofervidus phylogeny may represent unrecognized physiological and genomic diversity that calls for further investigation beyond the initial description of this group (Krukenberg et al., 2016). Investigating SEEP-SRB2, SEEP-SRB4, and *Ca.* Desulfofervidus showed that they are all phylogenetically distinct groups without a spectrum of close relatives among environmental clones as represented in NCBI GenBank (Figures 5–7). SEEP-SRB2, SEEP-SRB4, and *Ca.* Desulfofervidus all contain considerable internal phylogenetic diversity within their respective clades. We call attention to the occurrence of sulfur-disproportionating species and genera among the closest cultured relatives of SEEP-SRB2 and SEEP-SRB4 (Figures 6, 7), with sequence distances of up to ~8% between sulfur-disproportionating bacteria and SEEP-SRB2 and up to ~5% between sulfur-disproportionating bacteria and SEEP-SRB4 (Supplementary Data File 1, Sheets 3, 4); these mutually intertwined phylogenies suggest uncharted evolutionary complexity in seep environments where elemental sulfur and sulfur species of intermediate oxidation states are abundant (Jørgensen et al., 2019).

However, the chimera issues that we detected in sequences identified as *Ca.* Desulfofervidus, *Thermodesulfobacterium*, and *Beggiatoaceae*, underscore the need for phylogenetic analyses and alignment comparisons with high quality reference sequences to confirm the quality and identity of LoopSeq sequences, and the reliability of microbial community analyses. We also note that our DADA2 analysis of these sequences was not sufficient to detect these chimeras. Without manual verification of sequence alignments and scrutiny of isolated distal branches in phylogenetic clusters, problematic sequences can go undetected and create an illusion of diversity. Our observation of lineage-specific chimera issues calls for caution when using LoopSeq alone to investigate extreme and unusual bacterial groups. Further protocol development of LoopSeq should monitor this issue, and check sequence accuracy among a wide range of microbial target groups.

LoopSeq has successfully enabled a survey of the diversity of sulfur-cycling bacteria across a thermal and substrate gradient up to the current limit of hydrocarbon degradation (Figure 9). Due to the scope of this study, the diversity of archaea in surficial Guaymas Basin sediments was not investigated with LoopSeq. Future work may use LoopSeq to investigate potentially unknown archaeal diversity in habitats with extreme conditions or along environmental gradients, for example the strongly temperature-dependent archaeal communities in Guaymas Basin sediments (McKay et al., 2016; Ramírez et al., 2021). The phylogenetic resolution and range of archaeal lineages is limited by sequence coverage. Due to the limitations of popular primers, most available archaeal 16S rRNA gene sequences are 800 bp in length or less (Teske and Sørensen, 2008). High quality near full-length 16S rRNA gene sequence data, such as that provided by LoopSeq, would allow for an improved view of archaeal diversity.

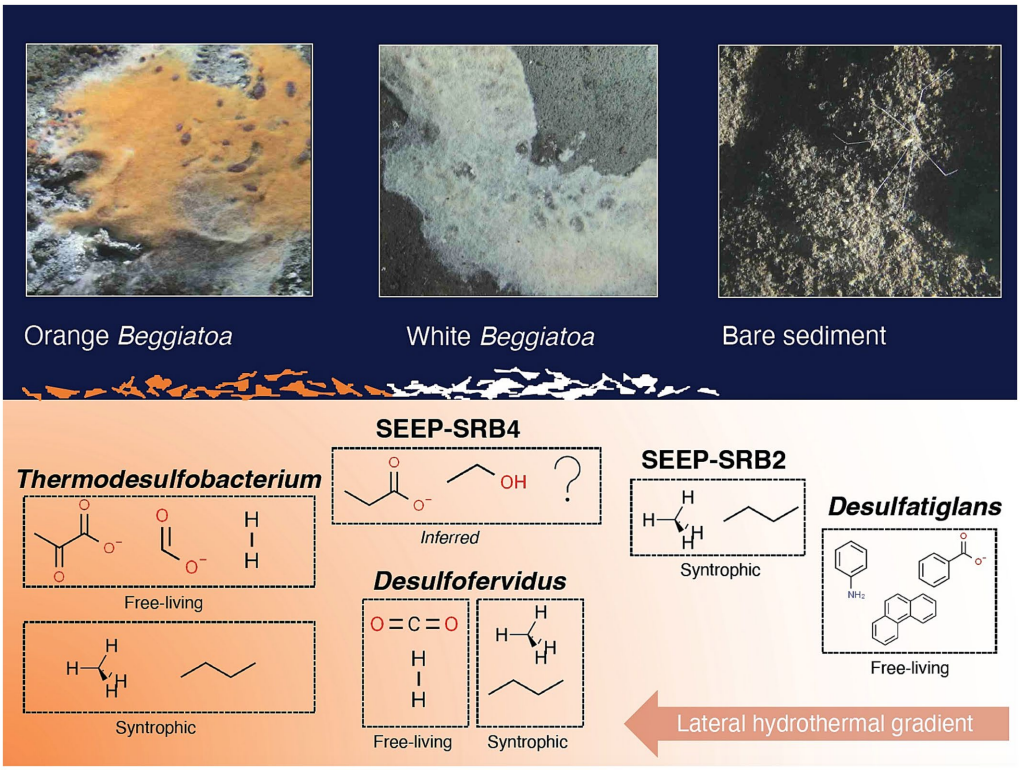

FIGURE 9
Conceptual figure of sulfur-cycling bacterial groups (with examples of preferred substrates) and their approximate distribution along a lateral hydrothermal gradient in surficial Guaymas Basin sediments. Examples of preferred substrates are shown for both free-living and syntrophic lifestyles, when applicable. Molecular structure images of the preferred substrates were obtained from chemspider.com. *Beggiatoaceae* mat and sediment close up images were captured with the bottom facing camera of HOV *Alvin* during Dive 4872.

Data availability statement

All sequence reads were submitted to the NCBI Sequence Read Archive (BioProject: PRJNA1105367). L-ASV sequences used in our phylogenetic trees are available in Supplementary Data Sheet 5 or via their NCBI GenBank accession number provided in each phylogenetic tree. All analysis code used in this study is available on the GitHub repository (https://github.com/moyn413/GuaymasLoopSeq/).

Author contributions

JH: Investigation, Writing – review & editing. JC: Investigation, Writing – review & editing. MM: Methodology, Software, Writing – review & editing. SR: Conceptualization, Funding acquisition, Project administration, Supervision, Writing – review & editing. AT: Funding acquisition, Project administration, Resources, Supervision, Writing – review & editing.

Funding

The author(s) declare that financial support was received for the research, authorship, and/or publication of this article. This study was supported by an NSF Biological Oceanography grant to AT (2048489), and by a grant from the Simons Foundation to SER (824763). Current research in the Teske lab is supported by NASA Exobiology (80NSSC24K1159).

Acknowledgments

We thank the R/V *Atlantis* and HOV *Alvin* crews for their exemplary support at sea, especially *Alvin* pilot Jefferson Grau for expert handling of the craft. We thank Chris Chambers for conducting the sulfide analyses. We thank Catherine Crowley and Adrián Fuentes for clean-up and quantification of the DNA. We thank Element Biosciences for their patience with our complex environmental samples. We thank Element Biosciences representative Dr. Caroline Obert for constructive communication that led to changes in the handling of low-biomass samples, and methods adaptation to improve DNA yield in low biomass samples.

Conflict of interest

The authors declare that the research was conducted in the absence of any commercial or financial relationships that could be construed as a potential conflict of interest.

The author(s) declared that they were an editorial board member of Frontiers, at the time of submission. This had no impact on the peer review process and the final decision.

Publisher's note

All claims expressed in this article are solely those of the authors and do not necessarily represent those of their affiliated organizations, or those of the publisher, the editors and the reviewers. Any product that may be evaluated in this article, or claim that may be made by its manufacturer, is not guaranteed or endorsed by the publisher.

Supplementary material

The Supplementary material for this article can be found online at: https://www.frontiersin.org/articles/10.3389/fmicb.2024.1491488/full#supplementary-material

References

Abellan-Schneyder, I., Siebert, A., Hofmann, K., Wenning, M., and Neuhaus, K. (2021). Full-length SSU rRNA gene sequencing allows species-level detection of bacteria, archaea, and yeasts present in milk. *Microorganisms* 9:1251. doi: 10.3390/microorganisms9061251

Barosa, B., Ferrillo, A., Selci, M., Giardina, M., Bastianoni, A., Correggia, M., et al. (2023). Mapping the microbial diversity associated with different geochemical regimes in the shallow-water hydrothermal vents of the Aeolian archipelago. *Italy. Front. Microbiol.* 14:1134114. doi: 10.3389/fmicb.2023.1134114

Benito Merino, D., Zehnle, H., Teske, A., and Wegener, G. (2022). Deep-branching ANME-1c archaea grow at the upper temperature limit of anaerobic oxidation of methane. *Front. Microbiol.* 13:988871. doi: 10.3389/fmicb.2022.988871

Callahan, B. J., Grinevich, D., Thakur, S., Balamotis, M. A., and Yehezkel, T. B. (2021). Ultra-accurate microbial amplicon sequencing with synthetic long reads. *Microbiome* 9:130. doi: 10.1186/s40168-021-01072-3

Callahan, B. J., McMurdie, P. J., Rosen, M. J., Han, A. W., Johnson, A. J. A., and Holmes, S. P. (2016). DADA2: high-resolution sample inference from Illumina amplicon data. *Nat. Methods* 13, 581–583. doi: 10.1038/nmeth.3869

Calvert, S. E. (1966). Origin of diatom-rich, varved sediments from the Gulf of California. *J. Geol.* 74, 546–565. doi: 10.1086/627188

Chanton, J., and Liptay, K. (2000). Seasonal variation in methane oxidation in a landfill cover soil as determined by an in situ stable isotope technique. *Global Biogeochem. Cycles* 14, 51–60.

Chiniquy, D., Barnes, E. M., Zhou, J., Hartman, K., Li, X., Sheflin, A., et al. (2021). Microbial community field surveys reveal abundant Pseudomonas population in sorghum rhizosphere composed of many closely related phylotypes. *Front. Microbiol.* 12:598180. doi: 10.3389/fmicb.2021.598180

Cline, J. D. (1969). Spectrophotometric determination of hydrogen sulfide in natural waters. *Limnol. Oceanogr.* 14, 454–458. doi: 10.4319/lo.1969.14.3.0454

De la Lanza-Espino, G., and Soto, L. A. (1999). Sedimentary geochemistry of hydrothermal vents in Guaymas Basin, gulf of California. *Mexico. Applied Geochemistry* 14, 499–510. doi: 10.1016/S0883-2927(98)00064-X

Dhillon, A., Lever, M., Lloyd, K., Albert, D. B., Sogin, M. L., and Teske, A. (2005). Methanogen diversity evidenced by molecular characterization of methyl coenzyme M reductase a (mcrA) genes (*mcr*A) in hydrothermal sediments of the Guaymas Basin. *Appl. Environ. Microbiol.* 71, 4592–4601. doi: 10.1128/AEM.71.8.4592-4601.2005

Dombrowski, N., Teske, A. P., and Baker, B. J. (2018). Expansive microbial metabolic versatility and biodiversity in dynamic Guaymas Basin hydrothermal sediments. *Nat. Commun.* 9:4999. doi: 10.1038/s41467-018-07418-0

Dowell, F., Cardman, Z., Dasarathy, S., Kellermann, M. Y., Lipp, J. S., Ruff, S. E., et al. (2016). Microbial communities in methane-and short chain alkane-rich hydrothermal sediments of Guaymas Basin. *Front. Microbiol.* 7:17. doi: 10.3389/fmicb.2016.00017

Edgcomb, V. P., Teske, A. P., and Mara, P. (2022). Microbial hydrocarbon degradation in Guaymas Basin—exploring the roles and potential interactions of fungi and sulfate-reducing bacteria. *Front. Microbiol.* 13:831828. doi: 10.3389/fmicb.2022.831828

Einsele, G., Gieskes, J. M., Curray, J., Moore, D. M., Aguayo, E., Aubry, M. P., et al. (1980). Intrusion of basaltic sills into highly porous sediments and resulting hydrothermal activity. *Nature* 283, 441–445. doi: 10.1038/283441a0

Engelen, B., Nguyen, T., Heyerhoff, B., Kalenborn, S., Sydow, K., Tabai, H., et al. (2021). Microbial communities of hydrothermal Guaymas Basin surficial sediment profiled at 2 millimeter-scale resolution. *Front. Microbiol.* 12:710881.

Felsenstein, J. (1985). Confidence limits on phylogenies: an approach using the bootstrap. *Evolution* 39, 783–791. doi: 10.2307/2408678

Finster, K., Liesack, W., and Thamdrup, B. O. (1998). Elemental sulfur and thiosulfate disproportionation by *Desulfocapsa sulfoexigens* sp. nov., a new anaerobic bacterium isolated from marine surface sediment. *Appl. Environ. Microbiol.* 64, 119–125. doi: 10.1128/AEM.64.1.119-125.1998

Friedrich, M., Springer, N., Ludwig, W., and Schink, B. (1996). Phylogenetic positions of Desulfofustis glycolicus gen. nov., sp. nov., and Syntrophobotulus glycolicus gen. nov., sp. nov., two new strict anaerobes growing with glycolic acid. *Int J Syst Bacteriol* 46, 1065–1069.

Goetz, F. E., and Jannasch, H. W. (1993). Aromatic hydrocarbon-degrading bacteria in the petroleum-rich sediments of the Guaymas Basin hydrothermal vent site: preference for aromatic carboxylic acids. *Geomicrobiol J.* 11, 1–18. doi: 10.1080/01490459309377928

Gutierrez, T., Biddle, J. F., Teske, A., and Aitken, M. D. (2015). Cultivation-dependent and cultivation-independent characterization of hydrocarbon-degrading bacteria in Guaymas Basin sediments. *Front. Microbiol.* 6:149000. doi: 10.3389/fmicb.2015.00695

Holler, T., Widdel, F., Knittel, K., Amann, R., Kellermann, M. Y., Hinrichs, K. U., et al. (2011). Thermophilic anaerobic oxidation of methane by marine microbial consortia. *ISME J.* 5, 1946–1956. doi: 10.1038/ismej.2011.77

Isaksen, M. F., and Teske, A. (1996). *Desulforhopalus vacuolatus* gen. Nov., sp. nov., a new moderately psychrophilic sulfate-reducing bacterium with gas vacuoles isolated from a temperate estuary. *Arch. Microbiol.* 166, 160–168. doi: 10.1007/s002030050371

Jochum, L. M., Schreiber, L., Marshall, I. P., Jørgensen, B. B., Schramm, A., and Kjeldsen, K. U. (2018). Single-cell genomics reveals a diverse metabolic potential of uncultivated *Desulfatiglans*-related Deltaproteobacteria widely distributed in marine sediment. *Front. Microbiol.* 9:384358. doi: 10.3389/fmicb.2018.02038

Jørgensen, B. B., Findlay, A. J., and Pellerin, A. (2019). The biogeochemical sulfur cycle of marine sediments. *Front. Microbiol.* 10:436320. doi: 10.3389/fmicb.2019.00849

Kawka, O. E., and Simoneit, B. R. (1990). Polycyclic aromatic hydrocarbons in hydrothermal petroleums from the Guaymas Basin spreading center. *Appl. Geochem.* 5, 17–27. doi: 10.1016/0883-2927(90)90032-Z

Kellermann, M. Y., Wegener, G., Elvert, M., Yoshinaga, M. Y., Lin, Y. S., Holler, T., et al. (2012). Autotrophy as a predominant mode of carbon fixation in anaerobic methane-oxidizing microbial communities. *Proc. Natl. Acad. Sci.* 109, 19321–19326. doi: 10.1073/pnas.1208795109

Kimura, M. (1980). A simple method for estimating evolutionary rates of base substitutions through comparative studies of nucleotide sequences. *J. Mol. Evol.* 16, 111–120. doi: 10.1007/BF01731581

Kleindienst, S., Herbst, F. A., Stagars, M., Von Netzer, F., Von Bergen, M., Seifert, J., et al. (2014). Diverse sulfate-reducing bacteria of the *Desulfosarcina/Desulfococcus* clade are the key alkane degraders at marine seeps. *ISME J.* 8, 2029–2044. doi: 10.1038/ismej.2014.51

Kniemeyer, O., Musat, F., Sievert, S. M., Knittel, K., Wilkes, H., Blumenberg, M., et al. (2007). Anaerobic oxidation of short-chain hydrocarbons by marine sulphate-reducing bacteria. *Nature* 449, 898–901. doi: 10.1038/nature06200

Knittel, K., Boetius, A., Lemke, A., Eilers, H., Lochte, K., Pfannkuche, O., et al. (2003). Activity, distribution, and diversity of sulfate reducers and other bacteria in sediments above gas hydrate (Cascadia margin, Oregon). *Geomicrobiol J.* 20, 269–294. doi: 10.1080/01490450303896

Knoblauch, C., Sahm, K., and Jørgensen, B. B. (1999). Psychrophilic sulfate-reducing bacteria isolated from permanently cold Arctic marine sediments: description of *Desulfofrigus oceanense* gen. Nov., sp. nov., *Desulfofrigus fragile* sp. nov., *Desulfofaba gelida* gen. Nov., sp. nov., *Desulfotalea psychrophila* gen. Nov., sp. nov. and *Desulfotalea arctica* sp. nov. *Int. J. Syst. Evol. Microbiol.* 49, 1631–1643. doi: 10.1099/00207713-49-4-1631

Konstantinidis, K. T., Rosselló-Móra, R., and Amann, R. (2017). Uncultivated microbes in need of their own taxonomy. *ISME J.* 11, 2399–2406. doi: 10.1038/ismej.2017.113

Krukenberg, V., Harding, K., Richter, M., Glöckner, F. O., Gruber-Vodicka, H. R., Adam, B., et al. (2016). *Candidatus* Desulfofervidus auxilii, a hydrogenotrophic sulfate-reducing bacterium involved in the thermophilic anaerobic oxidation of methane. *Environ. Microbiol.* 18, 3073–3091. doi: 10.1111/1462-2920.13283

Krukenberg, V., Riedel, D., Gruber-Vodicka, H. R., Buttigieg, P. L., Tegetmeyer, H. E., Boetius, A., et al. (2018). Gene expression and ultrastructure of meso- and thermophilic methanotrophic consortia. *Environ. Microbiol.* 20, 1651–1666. doi: 10.1111/1462-2920.14077

Lagostina, L., Frandsen, S., MacGregor, B. J., Glombitza, C., Deng, L., Fiskal, A., et al. (2021). Interactions between temperature and energy supply drive microbial communities in hydrothermal sediment communications. *Biology* 4:1006. doi: 10.1038/s42003-021-02507-1

Laso-Pérez, R., Wegener, G., Knittel, K., Widdel, F., Harding, K. J., Krukenberg, V., et al. (2016). Thermophilic archaea activate butane via alkyl-coenzyme M formation. *Nature* 539, 396–401. doi: 10.1038/nature20152

Lever, M. A., and Teske, A. (2015). Diversity of methane-cycling archaea in hydrothermal sediment investigated by general and group-specific PCR primers. *Appl. Environ. Microbiol.* 81, 1426–1441. doi: 10.1128/AEM.03588-14

Li, J., Su, L., Wang, F., Yang, J., Gu, L., Sun, M., et al. (2020). Elucidating the biomineralization of low-temperature hydrothermal precipitates with varying Fe, Si contents: indication from ultrastructure and microbiological analyses. *Deep-Sea Res. I Oceanogr. Res. Pap.* 157:103208. doi: 10.1016/j.dsr.2019.103208

Li, J., Zhou, H., Fang, J., Sun, Y., and Dasgupta, S. (2014). Microbial distribution in different spatial positions within the walls of a black sulfide hydrothermal chimney. *Mar. Ecol. Prog. Ser.* 508, 67–85. doi: 10.3354/meps10841

Lizarralde, D., Soule, S. A., Seewald, J. S., and Proskurowski, G. (2011). Carbon release by off-axis magmatism in a young sedimented spreading Centre. *Nat. Geosci.* 4, 50–54. doi: 10.1038/ngeo1006

Magen, C., Lapham, L. L., Pohlman, J. W., Marshall, K., Bosman, S., Casso, M., et al. (2014). A simple headspace equilibration method for measuring dissolved methane. *Limnol. Oceanogr. Methods* 12, 637–650. doi: 10.4319/lom.2014.12.637

Mara, P., Nelson, R. K., Reddy, C. M., Teske, A., and Edgcomb, V. P. (2022). Sterane and hopane biomarkers capture microbial transformations of complex hydrocarbons in young hydrothermal Guaymas Basin sediments. *Commun. Earth Environ.* 3:250. doi: 10.1038/s43247-022-00582-8

McKay, L., Klokman, V. W., Mendlovitz, H. P., LaRowe, D. E., Hoer, D. R., Albert, D., et al. (2016). Thermal and geochemical influences on microbial biogeography in the hydrothermal sediments of Guaymas Basin, Gulf of California. *Environ. Microbiol. Rep.* 8, 150–161. doi: 10.1111/1758-2229.12365

McKay, L. J., MacGregor, B. J., Biddle, J. F., Albert, D. B., Mendlovitz, H. P., Hoer, D. R., et al. (2012). Spatial heterogeneity and underlying geochemistry of phylogenetically diverse orange and white Beggiatoa mats in Guaymas Basin hydrothermal sediments. *Deep-Sea Res. I Oceanogr. Res. Pap.* 67, 21–31. doi: 10.1016/j.dsr.2012.04.011

McMurdie, P. J., and Holmes, S. (2013). Phyloseq: an R package for reproducible interactive analysis and graphics of microbiome census data. *PLoS One* 8:e61217. doi: 10.1371/journal.pone.0061217

Meyer, S., Wegener, G., Lloyd, K. G., Teske, A., Boetius, A., and Ramette, A. (2013). Microbial habitat connectivity across spatial scales and hydrothermal temperature gradients at Guaymas Basin. *Front. Microbiol.* 4:51282. doi: 10.3389/fmicb.2013.00207

Møller, M. H., Glombitza, C., Lever, M. A., Deng, L., Morono, Y., Inagaki, F., et al. (2018). D: L-amino acid modeling reveals fast microbial turnover of days to months in the subsurface hydrothermal sediment of Guaymas Basin. *Front. Microbiol.* 9:e967. doi: 10.3389/fmicb.2018.00967

Nelson, D. C., Wirsen, C. O., and Jannasch, H. W. (1989). Characterization of large, autotrophic Beggiatoa spp. abundant at hydrothermal vents of the Guaymas Basin. *Appl. Environ. Microbiol.* 55, 2909–2917. doi: 10.1128/aem.55.11.2909-2917.1989

Pérez Castro, S., Borton, M. A., Regan, K., Hrabe de Angelis, I., Wrighton, K. C., Teske, A. P., et al. (2021). Degradation of biological macromolecules supports uncultured microbial populations in Guaymas Basin hydrothermal sediments. *ISME J.* 15, 3480–3497. doi: 10.1038/s41396-021-01026-5

Qin, Q. L., Xie, B. B., Zhang, X. Y., Chen, X. L., Zhou, B. C., Zhou, J., et al. (2014). A proposed genus boundary for the prokaryotes based on genomic insights. *J. Bacteriol.* 196, 2210–2215. doi: 10.1128/jb.01688-14

Quast, C., Pruesse, E., Yilmaz, P., Gerken, J., Schweer, T., Yarza, P., et al. (2013). The SILVA ribosomal RNA gene database project: improved data processing and web-based tools. *Nucleic Acids Res.* 41, D590–D596. doi: 10.1093/nar/gks1219

R Core Team. (2022). R: A language and environment for statistical computing, Vienna, Austria. Available at: https://www.R-project.org/ (Accessed September 4, 2024).

Ramírez, G. A., Mara, P., Sehein, T., Wegener, G., Chambers, C. R., Joye, S. B., et al. (2021). Environmental factors shaping bacterial, archaeal and fungal community structure in hydrothermal sediments of Guaymas Basin, gulf of California. *PLoS One* 16:e0256321. doi: 10.1371/journal.pone.0256321

Ruff, S. E., Biddle, J. F., Teske, A. P., Knittel, K., Boetius, A., and Ramette, A. (2015). Global dispersion and local diversification of the methane seep microbiome. *Proc. Natl. Acad. Sci.* 112, 4015–4020. doi: 10.1073/pnas.1421865112

Rzhetsky, A., and Nei, M. (1995). Tests of applicability of several substitution models for DNA sequence data. *Mol. Biol. Evol.* 12, 131–151. doi: 10.1093/oxfordjournals.molbev.a040182

Salman, V., Amann, R., Girnth, A. C., Polerecky, L., Bailey, J. V., Høgslund, S., et al. (2011). A single-cell sequencing approach to the classification of large, vacuolated sulfur bacteria. *Syst. Appl. Microbiol.* 34, 243–259. doi: 10.1016/j.syapm.2011.02.001

Salman, V., Amann, R., Shub, D. A., and Schulz-Vogt, H. N. (2012). Multiple self-splicing introns in the 16S rRNA genes of giant sulfur bacteria. *Proc. Natl. Acad. Sci.* 109, 4203–4208. doi: 10.1073/pnas.1120192109

Salman, V., Bailey, J. V., and Teske, A. (2013). Phylogenetic and morphologic complexity of giant sulphur bacteria. *Antonie van Leeuwenhoek* 104, 169–186.

Schloss, P. D., and Handelsman, J. (2005). Introducing DOTUR, a computer program for defining operational taxonomic units and estimating species richness. *Appl. Environ. Microbiol.* 71, 1501–1506. doi: 10.1128/aem.71.3.1501-1506.2005

Schnell, S., and Schink, B. (1991). Anaerobic aniline degradation via reductive deamination of 4-aminobenzoyl-CoA in *Desulfobacterium anilini*. *Arch. Microbiol.* 155, 183–190. doi: 10.1007/BF00248615

Schutte, C. A., Teske, A., MacGregor, B. J., Salman-Carvalho, V., Lavik, G., Hach, P., et al. (2018). Filamentous giant *Beggiatoaceae* from the Guaymas Basin are capable of both denitrification and dissimilatory nitrate reduction to ammonium. *Appl. Environ. Microbiol.* 84:e02860-17. doi: 10.1128/AEM.02860-17

Slobodkin, A. I., Reysenbach, A. L., Slobodkina, G. B., Kolganova, T. V., Kostrikina, N. A., and Bonch-Osmolovskaya, E. A. (2013). *Dissulfuribacter thermophilus* gen. Nov., sp. nov., a thermophilic, autotrophic, sulfur-disproportionating, deeply branching deltaproteobacterium from a deep-sea hydrothermal vent. *Int. J. Syst. Evol. Microbiol.* 63, 1967–1971. doi: 10.1099/ijs.0.046938-0

Slobodkin, A. I., Slobodkina, G. B., Panteleeva, A. N., Chernyh, N. A., Novikov, A. A., and Bonch-Osmolovskaya, E. A. (2016). *Dissulfurimicrobium hydrothermale* gen. Nov., sp. nov., a thermophilic, autotrophic, sulfur-disproportionating deltaproteobacterium isolated from a hydrothermal pond. *Int. J. Syst. Evol. Microbiol.* 66, 1022–1026. doi: 10.1099/ijsem.0.000828

Sogin, M. L., Morrison, H. G., Huber, J. A., Welch, D. M., Huse, S. M., Neal, P. R., et al. (2006). Microbial diversity in the deep sea and the underexplored "rare biosphere". *Proc. Natl. Acad. Sci.* 103, 12115–12120. doi: 10.1073/pnas.0605127103

Song, M., Schubotz, F., Kellermann, M. Y., Hansen, C. T., Bach, W., Teske, A. P., et al. (2021). Formation of ethane and propane via abiotic reductive conversion of acetic acid in hydrothermal sediments. *Proc. Natl. Acad. Sci.* 118:e2005219118. doi: 10.1073/pnas.2005219118

Stackebrandt, E., and Goebel, B. M. (1994). Taxonomic note: a place for DNA-DNA reassociation and 16S rRNA sequence analysis in the present species definition in bacteriology. *Int. J. Syst. Evol. Microbiol.* 44, 846–849. doi: 10.1099/00207713-44-4-846

Stecher, G., Tamura, K., and Kumar, S. (2020). Molecular evolutionary genetics analysis (MEGA) for macOS. *Mol. Biol. Evol.* 37, 1237–1239. doi: 10.1093/molbev/msz312

Su, L., Teske, A. P., MacGregor, B. J., McKay, L. J., Mendlovitz, H., Albert, D., et al. (2023). Thermal selection of microbial communities and preservation of microbial function in Guaymas Basin hydrothermal sediments. *Appl. Environ. Microbiol.* 89:e0001823. doi: 10.1128/aem.00018-23

Suzuki, D., Li, Z., Cui, X., Zhang, C., and Katayama, A. (2014). Reclassification of *Desulfobacterium anilini* as *Desulfatiglans anilini* comb. nov. within *Desulfatiglans* gen. Nov., and description of a 4-chlorophenol-degrading sulfate-reducing bacterium, *Desulfatiglans parachlorophenolica* sp. nov. *Int. J. Syst. Evol. Microbiol.* 64, 3081–3086. doi: 10.1099/ijs.0.064360-0

Tamura, K., Nei, M., and Kumar, S. (2004). Prospects for inferring very large phylogenies by using the neighbor-joining method. *Proc. Natl. Acad. Sci.* 101, 11030–11035. doi: 10.1073/pnas.0404206101

Tamura, K., Stecher, G., and Kumar, S. (2021). MEGA11: molecular evolutionary genetics analysis version 11. *Mol. Biol. Evol.* 38, 3022–3027. doi: 10.1093/molbev/msab120

Teske, A. (2009). "Deep sea hydrothermal vents" in Desk encyclopedia of microbiology. ed. M. Schaechter (Cambridge, MA: Academic Press), 346–356.

Teske, A., de Beer, D., McKay, L., Tivey, M. K., Biddle, J. F., Hoer, D., et al. (2016). The Guaymas Basin hiking guide to hydrothermal mounds, chimneys and microbial mats: complex seafloor expressions of subsurface hydrothermal circulation. *Front. Microbiol.* 7:75.

Teske, A., Hinrichs, K. U., Edgcomb, V., de Vera Gomez, A., Kysela, D., Sylva, S. P., et al. (2002). Microbial diversity of hydrothermal sediments in the Guaymas Basin: evidence for anaerobic methanotrophic communities. *Appl. Environ. Microbiol.* 68, 1994–2007. doi: 10.1128/AEM.68.4.1994-2007.2002

Teske, A., McKay, L. J., Ravelo, A. C., Aiello, I., Mortera, C., Núñez-Useche, F., et al. (2019). Characteristics and evolution of sill-driven off-axis hydrothermalism in Guaymas Basin–the Ringvent site. *Sci. Rep.* 9:13847. doi: 10.1038/s41598-019-50200-5

Teske, A., and Sørensen, K. B. (2008). Uncultured archaea in deep marine subsurface sediments: have we caught them all? *ISME J.* 2, 3–18. doi: 10.1038/ismej.2007.90

Teske, A., Wegener, G., Chanton, J. P., Hoer, D., de Beer, D., Zhuang, G., et al. (2021). Microbial communities under distinct thermal and geochemical regimes in axial and off-axis sediments of Guaymas Basin. *Front. Microbiol.* 12:633649. doi: 10.3389/fmicb.2021.633649

Van de Peer, Y., Chapelle, S., and De Wachter, R. (1996). A quantitative map of nucleotide substitution rates in bacterial rRNA. *Nucleic Acids Res.* 24, 3381–3391. doi: 10.1093/nar/24.17.3381

Von Damm, K. L., Edmond, J. T., Measures, C. I., and Grant, B. (1985). Chemistry of submarine hydrothermal solutions at Guaymas Basin, gulf of California. *Geochim. Cosmochim. Acta* 49, 2221–2237. doi: 10.1016/0016-7037(85)90223-6

Waite, D. W., Chuvochina, M., Pelikan, C., Parks, D. H., Yilmaz, P., Wagner, M., et al. (2020). Proposal to reclassify the proteobacterial classes Deltaproteobacteria and Oligoflexia, and the phylum Thermodesulfobacteria into four phyla reflecting major functional capabilities. *Int. J. Syst. Evol. Microbiol.* 70, 5972–6016. doi: 10.1099/ijsem.0.004213

Wegener, G., Krukenberg, V., Riedel, D., Tegetmeyer, H. E., and Boetius, A. (2015). Intercellular wiring enables electron transfer between methanotrophic archaea and bacteria. *Nature* 526, 587–590. doi: 10.1038/nature15733

Welhan, J. A. (1988). Origins of methane in hydrothermal systems. *Chem. Geol.* 71, 183–198. doi: 10.1016/0009-2541(88)90114-3

Winkel, M., de Beer, D., Lavik, G., Peplies, J., and Mußmann, M. (2014). Close association of active nitrifiers with Beggiatoa mats covering deep-sea hydrothermal sediments. *Environ. Microbiol.* 16, 1612–1626. doi: 10.1111/1462-2920.12316

Yu, T., Cheng, L., Liu, Q., Wang, S., Zhou, Y., Zhong, H., et al. (2022). Effects of waterlogging on soybean rhizosphere bacterial community using V4, LoopSeq, and PacBio 16S rRNA sequence. *Microbiology Spectrum* 10, e02011–e02021. doi: 10.1128/spectrum.02011-21

Zehnle, H., Otersen, C., Benito Merino, D., and Wegener, G. (2023). Potential for the anaerobic oxidation of benzene and naphthalene in thermophilic microorganisms from the Guaymas Basin. *Front. Microbiol.* 14:1279865. doi: 10.3389/fmicb.2023.1279865

Zhou, J., Bruns, M. A., and Tiedje, J. M. (1996). DNA recovery from soils of diverse composition. *Appl. Environ. Microbiol.* 62, 316–322. doi: 10.1128/aem.62.2.316-322.1996

Zhuang, G. C., Heuer, V. B., Lazar, C. S., Goldhammer, T., Wendt, J., Samarkin, V. A., et al. (2018). Relative importance of methylotrophic methanogenesis in sediments of the Western Mediterranean Sea. *Geochim. Cosmochim. Acta* 224, 171–186. doi: 10.1016/j.gca.2017.12.024